Structural Determination of $NiC_nH_{2n}^+$ Ions in the Gas Phase Using Fourier Transform Mass Spectrometry Collision-Induced Dissociation

D. B. Jacobson and B. S. Freiser*

Contribution from the Department of Chemistry, Purdue University, West Lafayette, Indiana 47907. *Received May 27, 1982*

Abstract: In this paper we apply Fourier transform mass spectrometry to study the structures of $NiC_nH_{2n}^+$ complexes generated from reactions of Ni^+ with a variety of hydrocarbons and demonstrate that different isomeric structures can readily be distinguished both by a collision-induced dissociation and by specific ion–molecule reactions. Evidence is provided for four unique structures of $NiC_4H_8^+$ generated from reactions of Ni^+ with butane, hexane, 2,2-dimethylpropane, and cyclopentanone. Dehydrogenation reactions of Ni^+ with *n*-alkanes yield bis(olefin) complexes that are distinguishable from their isomeric monoalkene complexes. Ni^+ is found to be highly selective for cleaving internal bonds and highly selective against insertion into terminal C–C bonds. Dehydrogenation becomes more competitive with alkane elimination when β-hydride transfers from secondary carbons are involved instead of from primary carbons.

Reactions of gas-phase transition-metal ions with hydrocarbons has been the focus of recent investigations by ion cyclotron resonance (ICR) spectrometry[1-3] and ion beam techniques.[4-8] A variety of fundamental thermodynamic, kinetic, and mechanistic information about gas-phase organometallic chemistry may be obtained. A major emphasis of these studies is the formulation of reaction mechanisms that explain the formation of products. Cleavage of alkanes and dehydrogenation are the two most common processes observed in these studies. This is in contrast with solution-phase chemistry in which cleavage of carbon–carbon bonds is not as common as carbon–carbon bond formation by transition metals. The reason for this rich gas-phase chemistry is that the ion–molecule complex is activated with excess internal energy. This energy plus the metal–carbon and metal–hydrogen bond energies may be sufficient to allow for oxidative addition across carbon–carbon or carbon–hydrogen bonds. Oxidative addition of a metal ion across a carbon–carbon bond is postulated as the initial step in the cleavage of alkanes. This is followed by a β-hydride shift onto the metal and then onto the alkyl portion resulting in reductive elimination of an alkane and formation of a primary olefin–metal complex (Scheme I). Oxidative addition of a metal ion across a carbon–hydrogen bond is proposed as the initial step in dehydrogenation of alkanes. This is followed by a β-hydride shift onto the metal with reductive elimination of hydrogen (a 1,2-elimination process) and formation of an olefin–metal complex (Scheme II) where the olefin may be either cis or trans.

The determination of reaction mechanisms suffers from the fact that little is known about the structures of these products. Methods available to the gas-phase chemist for ion structure determination are increasing and include isotopic labeling, reactivity, photodissociation, and collision-induced dissociation (CID). Of these, collision-induced dissociation (CID) is among the most useful and

Scheme I

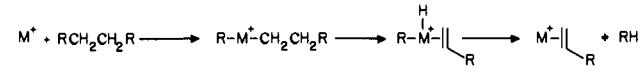

Scheme II

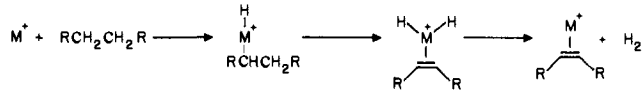

widely employed techniques for ion structure determination in the gas phase.[9] The CID technique consists of first selecting a particular ion and then accelerating the ion into a collision gas, thereby imparting internal energy into the ion, which induces fragmentation. This essentially yields a mass spectrum of the precursor ion from which structural information can be obtained. High kinetic energies (3–30 keV) are required to observe CID using mass-analyzed ion kinetic-energy spectrometry (MIKES) in reverse-geometry mass spectrometers.[10-12] Low-energy (<100 eV) CID was recently demonstrated by using a triple-quadrupole mass spectrometer.[13,14] This energy regime is readily accessible in an ion cyclotron resonance (ICR) spectrometer by irradiating a given ion at its cyclotron frequency in order to accelerate it. Recently we reported the first examples of collision-induced dissociation using a Nicolet prototype Fourier transform mass spectrometer (FT-MS).[15,16] The Fourier transform method as applied to ICR spectroscopy was first developed by Comisarow[17,18] and in general provides a number of real advantages over conventional ICR spectrometers, including high mass range, high resolution, and rapid data acquisition times. In addition, FT-MS is particularly compatible with laser ionization[2,3] in that a complete mass spectrum may be obtained from one laser pulse.

The application of CID to the study of transition metal ion chemistry should provide greater insight into ion structure and, therefore, reaction mechanisms. Ridge and Freas, for example,

(1) Allison, J.; Freas, R. B.; Ridge, D. P. *J. Am. Chem. Soc.* **1979**, *101*, 1332.
(2) Byrd, G. D.; Burnier, R. C.; Freiser, B. S. *J. Am. Chem. Soc.* **1982**, *104*, 3565.
(3) Burnier, R. C.; Byrd, G. D.; Freiser, B. S. *J. Am. Chem. Soc.* **1981**, *103*, 4360.
(4) Armentrout, P. B.; Beauchamp, J. L. *J. Chem. Phys.* **1981**, *74*, 2819.
(5) Armentrout, P. B.; Beauchamp, J. L. *J. Am. Chem. Soc.* **1981**, *103*, 784.
(6) Armentrout, P. B.; Halle, L. F.; Beauchamp, J. L. *J. Am. Chem. Soc.* **1981**, *103*, 6501.
(7) (a) Armentrout, P. B.; Halle, L. F.; Beauchamp, J. L. *J. Am. Chem. Soc.* **1981**, *103*, 6624. (b) Armentrout, P. B.; Beauchamp, J. L. *Ibid.* **1981**, *103*, 6628.
(8) Halle, L. F.; Armentrout, P. B.; Beauchamp, J. L. *Organometallics* **1982**, *1*, 963.
(9) Cooks, R. G. *Collision Spectrosc.* **1978**, 357.
(10) Kondrat, R. W.; Cooks, R. G. *Anal. Chem.* **1978**, *50*, 81A.
(11) McLafferty, R. W.; Bockhoff, F. M. *Anal. Chem.* **1978**, *50*, 69.
(12) Bozorgzadeh, M. H.; Morgan, R. P.; Beynon, J. H. *Analyst (London)* **1978**, *103*, 613.
(13) Yost, R. A.; Enke, C. G. *J. Am. Chem. Soc.* **1978**, *100*, 2274.
(14) Yost, R. A.; Enke, C. G. *Int. J. Mass Spectrom. Ion Phys.* **1979**, *30*, 127.
(15) Cody, R. B.; Freiser, B. S. *Int. J. Mass Spectrom. Ion Phys.* **1982**, *41*, 199.
(16) Cody, R. B.; Burnier, R. C.; Freiser, B. S. *Anal. Chem.* **1982**, *54*, 96.
(17) Parisod, G.; Comisarow, M. B. *Adv. Mass Spectrom.* **1980**, *8*, 216.
(18) Comisarow, M. B.; Parisod, G.; Grassi, V. *Chem. Phys. Lett.* **1978**, *57*, 413.

0002-7863/83/1505-0736$01.50/0

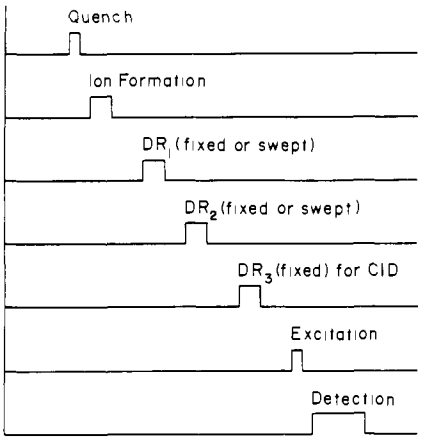

Figure 1. Typical sequence of events for the FT-MS CID experiment.

recently demonstrated the potential of CID in studies of $FeC_4H_{10}^+$ and $CrC_4H_{10}^+$ formed by reactions of $FeCO^+$ and $CrCO^+$ with butane using conventional reverse-geometry mass spectrometric techniques.[19]

In this paper we apply FT-MS to study the structures of $NiC_nH_{2n}^+$ complexes generated from reactions of Ni^+ with a variety of hydrocarbons and demonstrate that different isomeric structures can readily be distinguished both by collision-induced dissociation and by specific ion–molecule reactions.

Experimental Section

All experiments were performed on a prototype Nicolet FTMS-1000 ICR spectrometer previously described in detail[16] and equipped with a 1-in. cubic trapping cell situated between the poles of a Varian 15-in. electromagnet maintained at 0.9 T. The cell has been modified by drilling a $^1/_4$-in. diameter hole in one of the receiver plates, which permits irradiation with various light sources. A nickel foil of high purity was attached to the opposite receiver plate. Metal ions were generated by focusing the beam (530 nm, frequency doubled) of a Quanta Ray Nd:YAG laser onto the nickel foil. Details of the laser ionization technique have been described elsewhere.[3]

Chemicals were obtained commercially in high purity and were used as supplied except for multiple freeze–pump–thaw cycles to remove noncondensible gases. Sample pressures for the alkanes were on the order of 3×10^{-7} torr, with acetonitrile pressures being an order of magnitude less. Argon gas was used as the collision gas for the CID experiments at a total sample pressure of approximately 1×10^{-5} torr. A Bayard–Alpert ionization gauge was used to monitor pressure.

Details of the CID experiments have previously been discussed.[15,16] Figure 1 shows the timing sequence used in the CID experiments. A quench pulse that removes all ions present in the cell starts the experiment, followed by an ion formation pulse (a 20-ns laser pulse). This is followed by a 500–1000-ms reaction time. All ions except the ion of interest are then ejected from the cell (DR1 and DR2), followed by a CID pulse (DR3) of variable kinetic energy. There is an additional 25-ms delay after the CID pulse to allow for fragmentation, followed by detection to give a complete mass spectrum of the fragmentation products. The maximum translational energy acquired by the ion (in excess of thermal energy) is given by the relationship

$$E_{tr} = \frac{E_{RF}^2 e t^2}{8m} \qquad (1)$$

where e is the electronic charge (1.6×10^{-19} C to give E_{tr} in units of electron volts), m is the mass of the ion in kilograms, and E_{RF} is the amplitude of the irradiation frequency (26.9 V/m for all experiments). The time (t) of the irradiation frequency is then varied (0.060–0.700 ms) to vary the translational energy of the ions and, hence, the center of mass energy, which is related to the amount of internal energy an ion may obtain upon a single collision event at E_{tr}. The spread in ion kinetic energies is dependent on the total average kinetic energy and is approximately 5% at 30 eV, 10% at 10 eV, and 35% at 1 eV.[20]

The acetonitrile displacement reactions use a similar timing sequence to that of the CID experiments. The metal ion–alkane reaction product is initially formed after a trapping time of 500 ms; the unwanted ions are then ejected, followed by a second trapping time (variable, 250–5000 ms) to allow for displacement reactions with CH_3CN to occur.

(19) Freas, R. B.; Ridge, D. P. *J. Am. Chem. Soc.* **1980**, *102*, 7129.
(20) Huntress, W. T.; Mosesman, M. M.; Elleman, D. D. *J. Chem. Phys.* **1971**, *54*, 843.

Table I. Neutral Losses from CID of $NiC_4H_8^+$ Complexes[a,b]

structure	H_2	C_2H_4	C_4H_8
		X	X
	X		X
	X	X	X
			X

[a] CID fragments observed at 15-eV kinetic energy. [b] Argon added for total pressure of 1×10^{-5} torr.

Results and Discussion

In order to illustrate the experiment, results from $NiC_6H_{12}^+$ generated from Ni^+ in the presence of *n*-hexane are presented here. Figure 2a shows the FT mass spectrum derived from trapping Ni^+ for 500 ms in the presence of *n*-hexane at 3×10^{-7} torr and Ar at about 1×10^{-5} torr. Besides the $NiC_6H_{12}^+$ generated by reaction 2, a variety of other reaction products are observed. In

$$Ni^+ + C_6H_{14} \rightarrow NiC_6H_{12}^+ + H_2 \qquad (2)$$

exact analogy to the MS/MS approach, $NiC_6H_{12}^+$ was then selected by removing all of the other ions from the cell by using swept double-resonance ejection. This method simply accelerates the ions at their resonance frequency into the cell plates where they are annihilated. Figure 2b shows that this was successfully accomplished. Finally, in Figures 2c and 2d following the ejection of all the lower mass ions, a double-resonance pulse accelerates $^{58}NiC_6H_{12}^+$ to 5.6 and 15.4 eV, respectively, and its CID processes are clearly observed. That only the ^{58}Ni isotope is affected is particularly evident in the reduction of its intensity relative to the ^{60}Ni isotope shown in Figure 2d. Also, as expected, a greater degree of fragmentation is observed in Figure 2d, where the collision energy was greater, than in Figure 2c. The ratio of the CID products was found to be a strong function of the collision energy, and a plot of ion intensity vs. collision energy is shown in Figure 3a. For comparison, Figure 3b shows a similar plot for $NiC_6H_{12}^+$ generated by reaction 3 with *n*-octane. The plots

$$Ni^+ + n\text{-}C_8H_{18} \rightarrow NiC_6H_{12}^+ + C_2H_6 \qquad (3)$$

are significantly different and clearly indicate that the $NiC_6H_{12}^+$ species generated in reactions 2 and 3 are not the same. The interpretation of these results are discussed in greater detail below. As is evident from the above example, plots of ion intensity vs. collision energy are useful in summarizing the data and in observing trends and, therefore, will be used throughout this paper.

$NiC_4H_8^+$ Products. Ions corresponding to $NiC_4H_8^+$ were generated by reactions 4–7 and then selected from the other

$$Ni^+ + n\text{-}C_4H_{10} \rightarrow NiC_4H_8^+ + H_2 \qquad (4)$$

$$Ni^+ + n\text{-}C_nH_{2n+2} \rightarrow NiC_4H_8^+ + C_{n-4}H_{2n-6} \quad n = 5\text{–}9 \qquad (5)$$

$$Ni^+ + C(CH_3)_4 \rightarrow NiC_4H_8^+ + CH_4 \qquad (6)$$

$$Ni^+ + \text{cyclopentanone} \rightarrow NiC_4H_8^+ + CO \qquad (7)$$

products present by using the double-resonance ejection method described previously. These ions were then studied by CID and ion–molecule reactions with CH_3CN. The neutral losses observed from CID of the $NiC_4H_8^+$ ions are summarized in Table I. Each of the ions was subjected to identical conditions of 15-eV collision energy and 1×10^{-5} torr collision gas pressure. The results provide evidence for four unique structures.

Loss of C_2H_4 is the only fragmentation observed at low collision energies in the CID spectrum of $NiC_4H_8^+$ generated in reaction 4 while at higher collision energies loss of C_4H_8 is also observed.

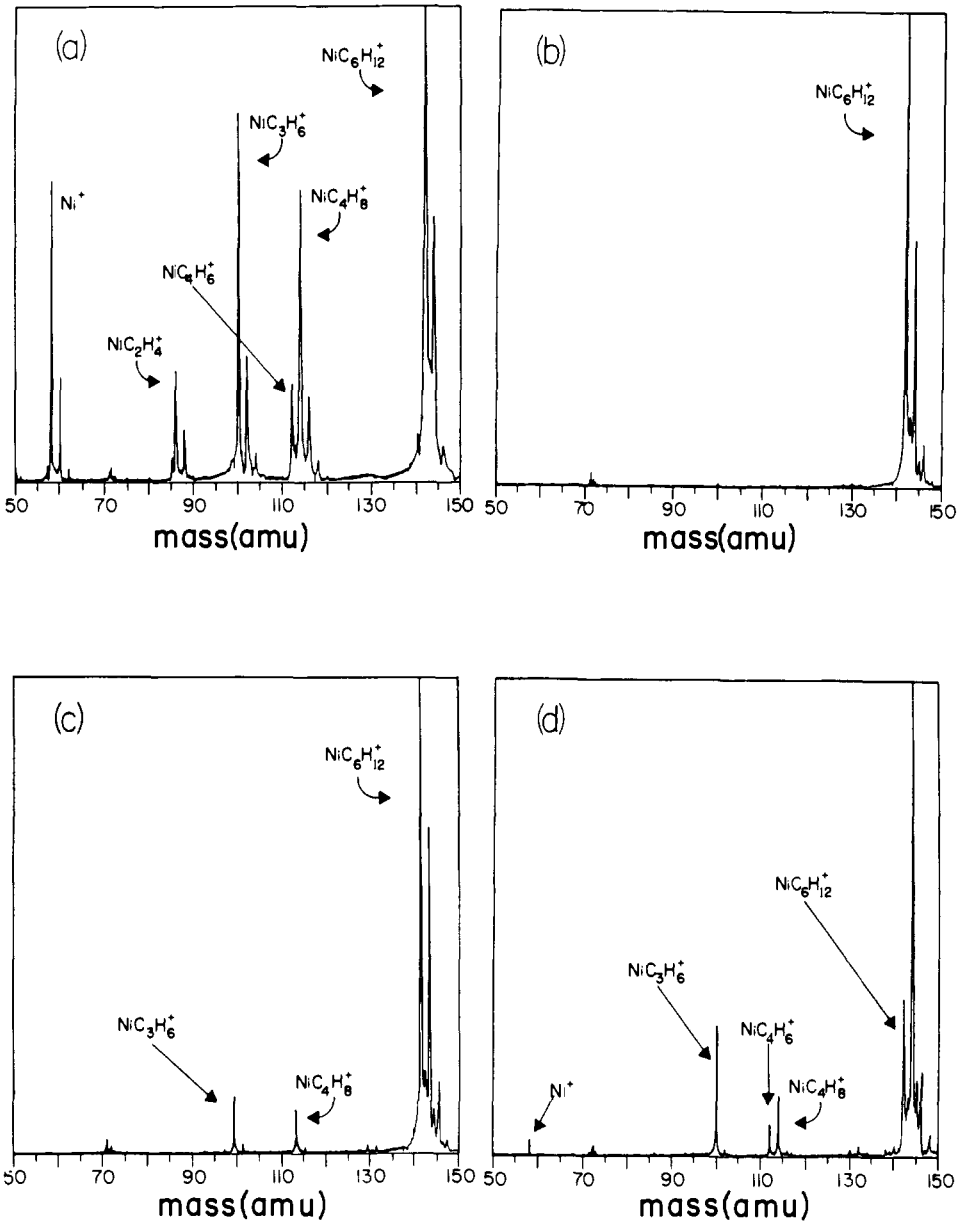

Figure 2. (a) Single-resonance mass spectrum resulting from laser emission of Ni^+ in the presence of *n*-hexane at approximately 3×10^{-7} torr and argon at a total pressure of 1×10^{-5} torr and a trapping time of 500 ms. (b) Same as (a) except all ions other than $NiC_6H_{12}^+$ have been ejected from the ICR cell by sweeping DR1 and DR2. (c) Same as (b) except following DR1 and DR2 the $^{58}NiC_6H_{12}^+$ species is accelerated to 5.6-eV kinetic energy and the CID fragments observed. (d) Same as (c) but the $^{58}NiC_6H_{12}^+$ species is accelerated to 15.4-eV kinetic energy and the CID fragments are observed.

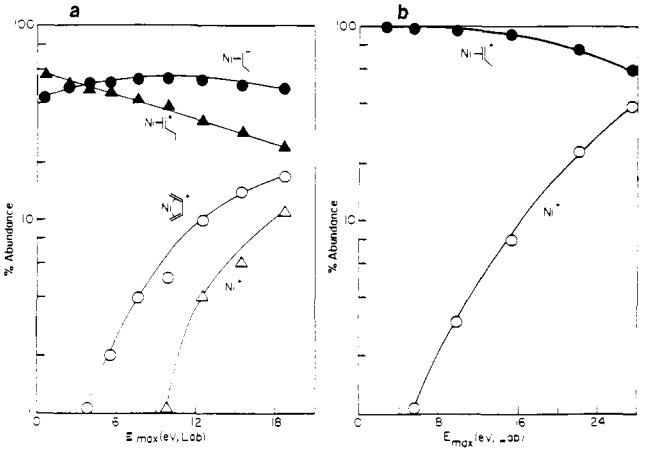

Figure 3. (a) CID product intensities vs. kinetic energy for $NiC_6H_{12}^+$ ions generated in reaction 2. (b) CID product intensities vs. kinetic energy for $NiC_6H_{12}^+$ ions generated in reaction 3.

Scheme III

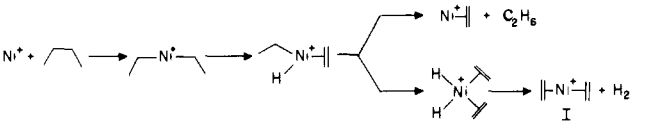

Loss of C_2H_4, however, dominates over the range of collision energies monitored. In addition to CID, this ion was also reacted with CH_3CN, and the sequential reaction 8 was observed. Both

$$NiC_4H_8^+ \xrightarrow{CH_3CN} Ni(C_2H_4)(CH_3CN)^+ \xrightarrow{CH_3CN} Ni(CH_3CN)_2^+ \quad (8)$$

sets of results provide evidence for the bis(olefin) structure I, which

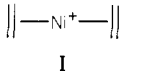

I

is consistent with the recent findings of Beauchamp et al.[21] Their

Scheme IV

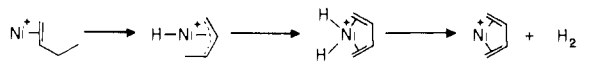

mechanism for the dehydrogenation of butane by Ni^+ is presented in Scheme III. Initially, Ni^+ oxidatively inserts into the internal C–C bond followed by β-hydride abstraction. Either reductive elimination of ethane occurs or a second β-hydride is abstracted, resulting in reductive elimination of H_2 producing the bis(olefin) complex I.

$NiC_4H_8^+$ is also produced as one of the major product ions from linear alkanes larger than butane by reaction 5. Dehydrogenation producing a nickel–butadiene complex along with loss of C_4H_8 are the only fragments observed in the CID spectrum of this ion, clearly eliminating the bis(olefin) structure. Instead, these results provide evidence for a primary butene bound to nickel, structure II. A dehydrogenation mechanism is outlined in Scheme IV.

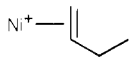

II

Oxidative addition of an allylic C–H bond to nickel forming an allyl metal hydride is the initial step. This is followed by β-hydride abstraction with subsequent reductive elimination of H_2 forming a butadiene complex. The allyl metal hydride has been proposed as an intermediate in solution-phase chemistry.[22-24]

Reaction 6, Ni^+ with 2,2-dimethylpropane, yields $NiC_4H_8^+$ as the only primary reaction product. The CID spectrum of this product shows only C_4H_8 loss, suggesting an isobutene structure III, distinguishable from the other two structures. This suggests

III

that considerable rearrangement is required for other fragmentations to occur.[7a]

Reaction 7, Ni^+ with cyclopentanone, produces $NiC_4H_8^+$ as a primary product.[25] Beauchamp et al. used ion–molecule reactions to distinguish this ion from the bis(olefin) structure I.[21] No ligand displacement reactions with HCN were observed, and while a metallocyclic structure IV was postulated, it was not proven

IV

to have a structure different from either II or III. The CID spectrum of this ion contains three fragmentations including loss of H_2, C_2H_4, and C_4H_8. Loss of H_2 and C_2H_4 occur at low kinetic energy while loss of C_4H_8 occurs only at high kinetic energy. Loss of C_2H_4 distinguishes this ion from having structures II or III. The metallocyclopentane structure (IV) is consistent with this fragmentation pattern. Dehydrogenation to form a butadiene complex could occur by a mechanism similar to that described for the dehydrogenation of II. Loss of C_2H_4 simply involves rearrangement to a bis(olefin) complex (I) followed by loss of C_2H_4. Loss of C_2H_4 has been observed in the thermal decomposition of nickelcyclopentanes in solution.[26,27]

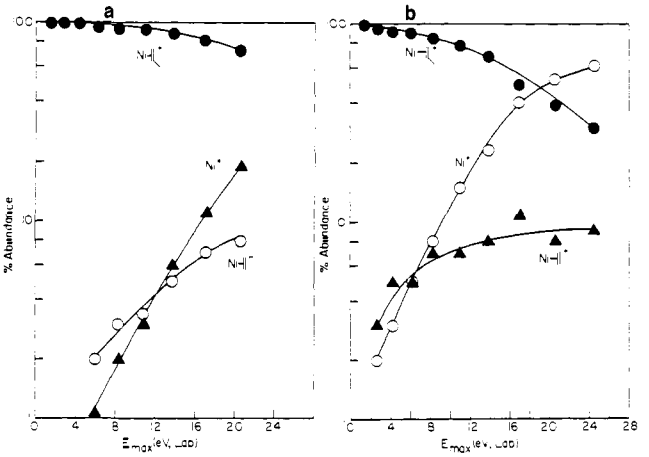

Figure 4. (a) CID product ion intensities vs. kinetic energy for $NiC_5H_{10}^+$ ions generated in reaction 9. (b) CID product ion intensities vs. kinetic energy for $NiC_5H_{10}^+$ ions generated in reaction 10.

Scheme V

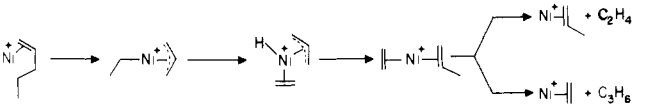

$NiC_5H_{10}^+$ Products. Ions corresponding to $NiC_5H_{10}^+$ were generated by reactions 9 and 10. The plots of ion intensity vs.

$$Ni^+ + n\text{-}C_5H_{12} \rightarrow NiC_5H_{10}^+ + H_2 \quad (9)$$

$$Ni^+ + n\text{-}C_8H_{18} \rightarrow NiC_5H_{10}^+ + C_3H_8 \quad (10)$$

collision energy for $NiC_5H_{10}^+$ from reactions 9 and 10 are shown in Figure 4. As in the butane case, the fragmentation pattern for the dehydrogenation product (reaction 9) is consistent with the bis(olefin) complex V, suggesting initial insertion of Ni^+ into

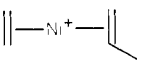

V

the internal C–C bond. Loss of C_2H_4 and C_3H_6 to produce $NiC_3H_6^+$ and $NiC_2H_4^+$, respectively, are the only fragmentations observed at low kinetic energy. At higher kinetic energy, loss of C_5H_{10} to produce Ni^+ is observed. Loss of C_2H_4 dominates over loss of C_3H_6 at all kinetic energies, with the greatest dominance at the lowest collision energies. This is consistent with the fact that larger alkenes are more strongly bound to metal ion centers than smaller alkenes, and, hence, smaller alkenes will be preferentially cleaved from the complex.[28] Finally, displacement reaction 11, $NiC_5H_{10}^+$ by CH_3CN, confirms the ethene–propene

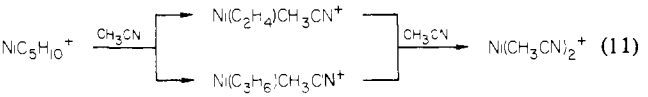

$$NiC_5H_{10}^+ \xrightarrow{CH_3CN} \begin{matrix} Ni(C_2H_4)CH_3CN^+ \\ Ni(C_3H_6)CH_3CN^+ \end{matrix} \xrightarrow{CH_3CN} Ni(CH_3CN)_2^+ \quad (11)$$

structure. Acetonitrile initially displaces either C_2H_4 or C_3H_6 in roughly equal amounts. Ultimately both alkenes are displaced as written in reaction 11 to yield $Ni(CH_3CN)_2^+$.

Reaction of Ni^+ with octane produces $NiC_5H_{10}^+$ as a primary reaction product (reaction 10). Presumably this ion consists of a primary pentene bound to Ni^+ (structure VI) (Scheme I). The

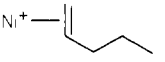

VI

(21) Halle, L. F.; Houriet, R.; Kappes, M.; Staley, R. H.; Beauchamp, J. L. *J. Am. Chem. Soc.* **1982**, *104*, 6293.
(22) Tulip, T. H.; Ibers, J. A. *J. Am. Chem. Soc.* **1981**, *101*, 4201.
(23) Ephritikhine, M.; Green, M. L. H.; MacKenzie, R. E. *J. Chem. Soc., Chem. Commun.* **1976**, 619.
(24) Byrne, J. W.; Blaser, H. U.; Osborn, J. A. *J. Am. Chem. Soc.* **1975**, 97, 3871.
(25) Studies of the reaction of Ni^+ with ^{18}O-labeled cyclopentanone indicate that decarbonylation is the major process in which a neutral with 28 amu using the unlabeled reactant is eliminated, accounting for greater than 90% of the product. A minor process results in loss of ethene from the 3,4 sites on the ring (Kalmbach, K. A.; Ridge, D. P., unpublished results).
(26) Grubbs, R. H.; Miyashita, A.; Liu, M.; Burk, P. *J. Am. Chem. Soc.* **1978**, *100*, 2418.
(27) Braterman, P. S. *J. Chem. Soc., Chem. Commun.* **1979**, 70.
(28) Kappes, M. M.; Staley, R. H. *J. Am. Chem. Soc.* **1982**, *104*, 1813.

Scheme VI

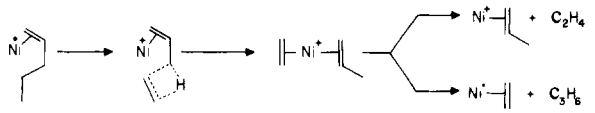

variation in CID product ion intensity vs. collision energy (Figure 4b) for this ion is similar to that of the bis(olefin) structure V. Loss of C_2H_4 and C_3H_6 occur at low kinetic energies, with loss of C_2H_4 dominating at all kinetic energies. Loss of C_5H_{10} to form Ni^+, however, occurs at a lower kinetic energy for VI than V and also is more dominant at higher kinetic energies. Scheme V presents a possible mechanism for loss of C_2H_4 and C_3H_6 in analogy to the mechanism for reaction of Co^+ with 1-pentene.[7a] The initial step involves oxidative addition to the allylic C–C bond to produce an allyl–alkyl complex. This is followed by β-hydride transfer across the metal to form a propene–ethene complex that reductively eliminates ethene or propene. An alternative mechanism involves transfer of hydrogen from the terminal methyl group to the allyl carbon via a four-centered intermediate to produce a bis(olefin) complex that reductively eliminates ethene or propene (Scheme VI).[29] A metallocyclobutane intermediate may also be involved, but it would not be as facile as either of the above mechanisms.[7a] One consequence of these results is that, regardless of the specific mechanism, $NiC_5H_{10}^+$ ions formed from reaction 10 with sufficient internal energy may rearrange to the bis(olefin) structure. Displacement reactions of VI by CH_3CN, however, provide further evidence for the presence of a stable primary pentene–Ni^+ structure. Initial attachment of CH_3CN to VI produces an activated complex that either loses mainly C_2H_4 (reaction 12) or remains long-lived (reaction 13), probably due

$$NiC_5H_{10}^+ + CH_3CN \rightarrow [Ni(C_5H_{10})(CH_3CN)^+]^* \rightarrow Ni(C_3H_6)(CH_3CN)^+ + C_2H_4 \quad (12)$$

$$NiC_5H_{10}^+ + CH_3CN \rightarrow [Ni(C_5H_{10})(CH_3CN)^+]^* \rightarrow Ni(C_5H_{10})(CH_3CN)^+ \quad (13)$$

to IR radiative stabilization.[30] The products in reactions 12 and 13 go on to form $Ni(CH_3CN)_2^+$. The observation of the stabilized intermediate in reaction 13, together with a reduced abundance of $Ni(C_2H_4)(CH_3CN)^+$, distinguishes structure VI from the bis(olefin) complex V. It is evident, however, that cleavage products do not necessarily infer attachment of that species directly to the metal.

$NiC_6H_{12}^+$ Products. Ions corresponding to $NiC_6H_{12}^+$ were generated as discussed earlier by reactions 2 and 3. The CID spectrum of $NiC_6H_{12}^+$ formed by the dehydrogenation of hexane (reaction 2) indicates the presence of two bis(olefin) structures VII and VIII as expected from initial insertion of Ni^+ into the

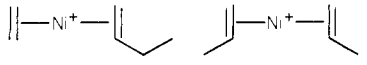

VII VIII

two interior C–C bonds. The distribution of fragments as a function of collision energy is shown in Figure 3a. Loss of C_2H_4 and C_3H_6, presumably from structures VII and VIII, respectively, are observed at low kinetic energy to produce $NiC_4H_8^+$ (57 ± 10%) and $NiC_3H_6^+$ (43 ± 10%). At higher energies the $NiC_4H_8^+$ fragment has sufficient internal energy for dehydrogenation to occur, forming a Ni^+–butadiene complex as expected from a primary butene bound to Ni^+ (structure II), discussed earlier. Also, a small amount of Ni^+ is observed at high kinetic energies. Displacement reactions with acetonitrile once again confirm the CID results. Figure 5a shows the temporal variation of these reactions. Initially, CH_3CN displaces C_3H_6 from VIII to produce

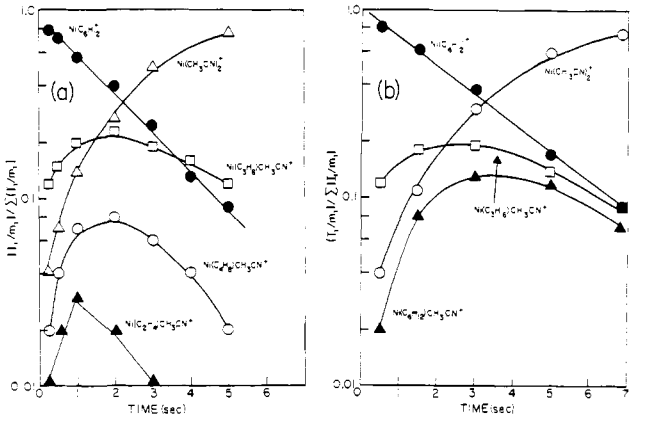

Figure 5. (a) Temporal variation for the reaction of $NiC_6H_{12}^+$ ions generated in reaction 2 with CH_3CN. (b) Temporal variation for the reaction of $NiC_6H_{12}^+$ ions generated in reaction 3 with CH_3CN.

Table II. Predicted Fractional Losses of X_2 (X = H, D) in the Reactions of Ni^+ with Deuterated *n*-Alkanes (Experimental Numbers are in Parentheses)[a]

alkane	H_2	loss of HD	D_2
butane-**1**,**1**,1,4,4,4-d_6			1.0 (1.0)
pentane-**1**,**1**,**1**,**5**,**5**,**5**-d_6		1.0 (1.0)	
pentane-**2**,**2**,3,3,4,4-d_6		1.0 (1.0)	
hexane-**1**,1,1,6,6,6-d_6	0.43 (0.48)	0.57 (0.52)	
hexane-**2**,**2**,**5**,**5**-d_4	0.57 (0.55)		0.43 (0.45)
hexane-3,3,4,4-d_4	0.43 (0.47)	0.57 (0.53)	
hexane-**1**,**1**,6,6-d_4	0.62 (0.71)	0.38 (0.29)	
hexane-3,**3**-d_2	0.72 (0.80)	0.28 (0.20)	

[a] Experimental numbers from ref 21.

$Ni(C_3H_6)(CH_3CN)^+$ followed by a second displacement to give $Ni(CH_3CN)_2^+$ (reaction 14). Acetonitrile displaces either C_2H_4

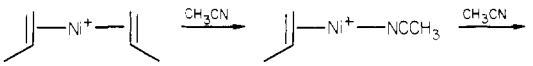

VIII

$Ni(CH_3CN)_2^+$ (14)

or C_4H_8 from VII to produce $Ni(C_4H_8)(CH_3CN)^+$ and $Ni(C_2H_4)(CH_3CN)^+$, and a subsequent reaction with CH_3CN forms $Ni(CH_3CN)_2^+$ (reaction 15). No direct attachment of acetonitrile

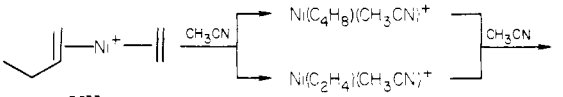

VII

$Ni(CH_3CN)_2^+$ (15)

is observed. Table II shows the predicted fractional loss of X_2 (X = H, D) in the dehydrogenation of deuterated linear alkanes and compares this to experimental results obtained by Beauchamp.[21] The fractional distribution of structures VII and VIII are used to obtain the predicted values in the hexane case. As can be seen, the predicted and observed values are in good agreement.

The variation of CID product ion intensity as a function of collision energy for $NiC_6H_{12}^+$, obtained by reaction of Ni^+ with octane (eq 3) as shown in Figure 3b, is markedly different than the previous example in that it contains only the loss of C_3H_6 at low collision energies. This loss dominates at higher energies as well, where loss of C_6H_{12} to form Ni^+ is also observed. These results are consistent with a Ni^+–hexene structure IX. Loss of

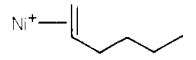

IX

C_3H_6 could be explained by either Scheme III or IV. Scheme III would require oxidative addition into the allylic C–C bond.

(29) Hydrogen transfer involving a four-membered intermediate has been proposed, see, for example: (a) Gamble, A. A.; Gilert, J. R.; Tillett, J. G. *Org. Mass Spectrom.* **1971**, *5*, 1093. (b) Uccella, N.; Howe, I.; Williams, D. H. **1972**, *6*, 229. (c) Tomer, K. B.; Djerassi, C. *Tetrahedron* **1973**, *29*, 3491.
(30) Woodin, R. L.; Beauchamp, J. L. *Chem. Phys.* **1979**, *41*, 1.

Table III. Percentages of Neutral Products Lost in Primary Reactions of Ni^+ with Linear Alkanes[a-c]

	neutrals lost								
alkane	H_2	CH_4	C_2H_6	C_3H_8	C_4H_{10}	C_5H_{12}	H_2 (C_2H_6)	H_2 (C_3H_8)	H_2 (C_4H_{10})
propane	20	80							
butane	12	4	84						
pentane	37	2	44	17					
hexane	36		22	27	8		7		
heptane	24		12	32	22	5		5	
octane	38		6	34	15	6			1

[a] Alkane pressure ~3×10^{-7} torr. [b] Argon added for a total pressure of 1×10^{-5} torr. [c] All numbers are ±10% of absolute.

Scheme IV would involve hydrogen transfer from the 5-carbon to the allyl carbon via a four-membered intermediate. In both cases, a bis(propene) complex is produced that eliminates propene and again suggests that any $NiC_6H_{12}^+$ formed from reaction 3 with sufficient internal energy may rearrange to a bis(propene) complex. Displacement reactions with acetonitrile are, however, consistent with IX (Figure 5b). Acetonitrile is observed to attach directly to IX to produce an activated complex that either loses C_3H_6 (reaction 16) or becomes stabilized (reaction 17). Again,

$$NiC_6H_{12}^+ \xrightarrow{CH_3CN} [Ni(C_6H_{12})(CH_3CN)^+]^* \rightarrow Ni(C_3H_6)(CH_3CN)^+ + C_3H_6 \quad (16)$$

$$NiC_6H_{12}^+ \xrightarrow{CH_3CN} [Ni(C_6H_{12})(CH_3CN)^+]^* \rightarrow Ni(C_6H_{12})(CH_3CN)^+ \quad (17)$$

observation of the stabilized intermediate in reaction 17 serves to distinguish structure IX from the bis(olefin) structures VII and VIII. The products in reactions 16 and 17 go on to produce $Ni(CH_3CN)_2^+$.

$NiC_7H_{14}^+$ Products. $NiC_7H_{14}^+$ ions were generated by reaction of Ni^+ with *n*-heptane (eq 18). As shown in Figure 6, which plots

$$Ni^+ + n\text{-}C_7H_{16} \rightarrow NiC_7H_{14}^+ + H_2 \quad (18)$$

fragment ion abundance vs. kinetic energy, at low energies, loss of C_3H_6 dominates over loss of C_2H_4 to produce $NiC_4H_8^+$ (85 ± 10%) and $NiC_5H_{10}^+$ (15 ± 10%), suggesting structures X and XI, respectively. At higher kinetic energies, the $NiC_3H_6^+$ fragment

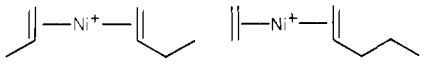

X XI

appears and increases while $NiC_5H_{10}^+$ decreases, indicating a coupling of these two fragments as expected for a primary pentene structure VI. In addition, however, structure X can also directly lose butene to produce $NiC_3H_6^+$. The $NiC_4H_8^+$ fragment dehydrogenates to form the butadiene–Ni^+ complex as expected for a primary butene structure II. Loss of C_7H_{14} to produce Ni^+ was not observed over the energies studied.

$NiC_8H_{16}^+$ Products. Dehydrogenation of *n*-octane by Ni^+ produces $NiC_8H_{16}^+$ (reaction 19). The CID fragments of this

$$Ni^+ + n\text{-}C_8H_{18} \rightarrow NiC_8H_{16}^+ + H_2 \quad (19)$$

ion as a function of kinetic energy are shown in Figure 7 and provide evidence for structures XII and XIII. At low kinetic

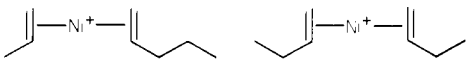

XII XIII

energies, XII loses C_3H_6 to produce $NiC_5H_{10}^+$. At higher energy, the $NiC_5H_{10}^+$ ion fragment intensity decreases while $NiC_3H_6^+$ appears and increases, indicating that these two fragment ions, as expected, are coupled. Structure XIII loses C_4H_8 at low energies to produce $NiC_4H_8^+$, which dehydrogenates at higher kinetic energies to produce $NiC_4H_6^+$, the butadiene complex. The data suggest 55 ± 10% structure XII and 45 ± 10% structure XIII.

Selective C–C Bond Cleavage. Product distributions for the reactions of Ni^+ with several linear alkanes, C_3 through C_8, are presented in Table III. These results together with the dehydrogenation product distributions (determined by CID) are used to determine the particular C–C bond cleaved by Ni^+ (Table IV). A comparison is made with nonselective insertion. As can be seen, Ni^+ is highly selective against insertion into terminal C–C bonds. This is not surprising since terminal C–C bonds are roughly 3 kcal/mol stronger than internal C–C bonds. The selectivity of

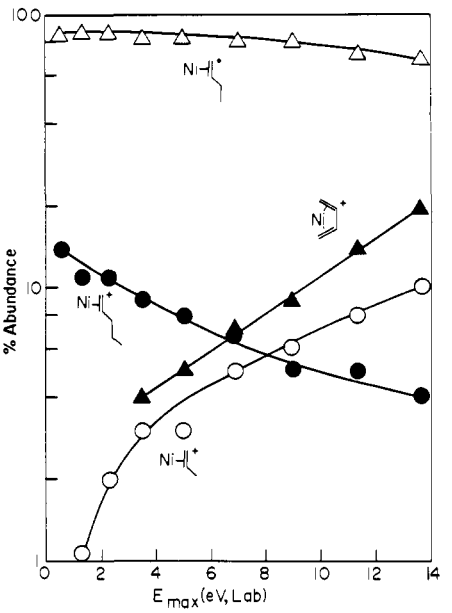

Figure 6. CID product ion intensities vs. kinetic energy for $NiC_7H_{14}^+$ ions generated in reaction 18.

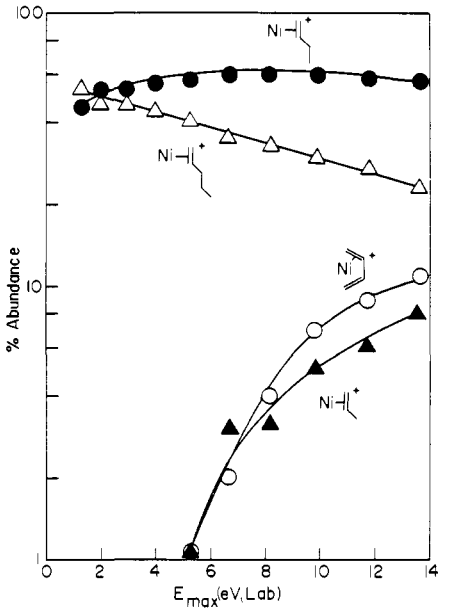

Figure 7. CID product ion intensities vs. kinetic energy for $NiC_8H_{16}^+$ ions generated in reaction 19.

Table IV. Observed Carbon-Bond Cleavage by Ni^+ Compared with Nonselective Insertion[a,b]

	carbon bond cleaved			
	1	2	3	4
	OBS = 4	96		
	PRE = 67	33		
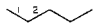	OBS = 2	98		
	PRE = 50	50		
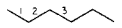	OBS = 0	54	46	
	PRE = 40	40	20	
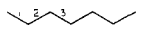	OBS = 0	21	79	
	PRE = 33	33	33	
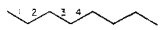	OBS = 0	6	61	33
	PRE = 28.5	28.5	28.5	14.5

[a] OBS = observed relative intensity. PRE = predicted relative intensities based on nonselective insertion. [b] Dehydrogenation products are included.

Table V. Fraction of Dehydrogenation vs. Alkane Loss (H_2/Alkane Loss) for Each Carbon Bond Cleaved

	carbon bond cleaved			
alkane	1	2	3	4
	0	0.14		
	0	0.61		
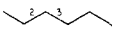	0	0.55	0.57	
	0	0.17	0.35	
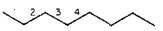	0	0	0.52	1.07

Ni^+ for the most internal C-C bond, however, is surprising. In the case of octane, the β-carbon bond is cleaved one-tenth as often as the adjacent internal carbon bond, which, in turn, is cleaved as often as the central bond. The energy difference of these three internal bonds is less than 1 kcal/mol.[31] It is interesting to note that this chemistry is in contrast to the nonselective behavior observed for Fe^+.[2]

As Scheme III indicates, dehydrogenation by sequential β-hydride transfers is competitive with reductive elimination of an alkane.[32] Table V lists the ratio of dehydrogenation to alkane loss for each carbon bond cleaved for several linear alkanes, C_4 through C_8, by using data from Tables III and IV. The results suggest that dehydrogenation becomes more competitive with alkane elimination when β-hydride transfers from secondary carbons are involved instead of from primary carbons. This is expected since secondary β-hydride transfers are in general more facile than primary β-hydride transfers.[5]

Conclusion

The $NiC_4H_8^+$ ion generated in the reaction of Ni^+ with cyclopentanone (reaction 7) has the metallocyclopentane structure IV. Beauchamp et al.[21] demonstrated that Ni^+ dehydrogenates butane to produce a bis(olefin) complex, I. A metallocycle is not involved in the dehydrogenation of butane since a metallocyclopentane generated from reaction 4 would have 11 kcal/mol less internal energy than the same species generated in reaction 7 (assuming no excess energy is carried away by the neutrals), and hence a metallocycle from reaction 4 would not be expected to fragment into a bis(olefin) complex as observed.[33] Beauchamp et al. first proposed that Ni^+ dehydrogenates butane by a highly specific 1,4-elimination process (Scheme III).[21] Our results substantiate this mechanism. In addition, we have expanded this study to include linear alkanes through octane, and all are dehydrogenated by Ni^+ by a mechanism similar to Scheme III. An interesting observation of this mechanism is that it requires β-hydride transfer to compete with reductive elimination of alkanes.

One possible complication in this study is that the $NiC_nH_{2n}^+$ ions formed initially by H_2 or alkane loss may retain enough internal energy to cause rearrangement prior to analysis by CID. Specifically, in the dehydrogenation reactions 2, 9, and 18, $NiC_nH_{2n}^+$ could be formed following an initial C–H insertion (Scheme II) with enough internal energy to rearrange to a bis(olefin) structure in a manner similar to Schemes V or VI. While our study cannot totally rule out this possibility, there are several compelling reasons to believe that this is not the case. First, it has been shown that Ni^+ dehydrogenates butane exclusively by a 1,4 elimination with no evidence for an initial insertion into C–H bonds. Second, it is more favorable thermodynamically for Ni^+ to insert into C–C bonds than C–H bonds in linear alkanes, and it becomes even more so as the chain length is increased. Both of these points suggest that the dehydrogenation mechanism determined for butane in Scheme III is generally applicable to the larger alkanes. The arguments are not as strong for $NiC_nH_{2n}^+$ ions generated by alkane loss, and some rearrangement may occur to form bis(olefin) complexes in these cases. Displacement reactions with CH_3CN, however, provide direct evidence for the presence of unrearranged primary olefin complexes.

Beauchamp et al. proposed that thermochemistry is the factor that allows Ni^+ to insert into C–C bonds but not C–H bonds in linear alkanes larger than propane.[21] However, Ni^+ also is observed to dehydrogenate propane. This dehydrogenation occurs by a different mechanism than that for larger alkanes and only involves insertion into C–H bonds, a 1,2-elimination process (Scheme II). The reaction of Ni^+ with propane is considerably slower than that for the larger alkanes, which approach the Langevin rate. This may allow insertion into C–H bonds to compete with insertion into C–C bonds. In general, however, insertion into C–C bonds by Ni^+ is more facile (higher frequency factor, lower activation energies) than that for insertion into C–H bonds.

Ethene and propene both yield simple cleavages as the only CID fragments observed when bound to Ni^+. A primary butene bound to nickel can dehydrogenate to form a butadiene complex as a CID product. However, no nickel–alkadiene products are observed in the CID spectrum of olefins larger than butene bound to nickel. Primary pentenes or primary hexenes bound to nickel rearrange to eliminate C_2H_4 or C_3H_6. In cases where there is a bis(olefin) complex, direct cleavage of one of the olefins is the initial fragmentation observed. Additional fragmentation can then be observed with the remaining olefin, such as simple cleavage, dehydrogenation of butene, or rearrangement of pentene or hexene followed by loss of C_2H_4 or C_3H_6. Therefore, caution must be exercised in interpreting the CID spectra of organometallic ions since the observation of cleavage products does not necessarily infer attachment of that species directly on the metal. It is evident, however, that CID is a powerful technique for determining the structures of organometallic ions yielding information about fundamental chemical behavior.

Acknowledgment is made to the Department of Energy (DE-AC02-80ER10689) for supporting this research and the National Science Foundation (CHE-8002685) for providing funds to purchase the FTMS.

Registry No. I, 83984-52-5; II, 83984-53-6; III, 83984-55-8; IV, 83984-54-7; V, 83984-56-9; VI, 83984-57-0; VII, 83984-58-1; VIII, 80719-66-0; IX, 83984-59-2; X, 83984-60-5; XI, 83984-61-6; XII, 83984-62-7; XIII, 80719-58-0; Ni^+, 14903-34-5; CH_3CN, 75-05-8; propane, 74-98-6; butane, 106-97-8; pentane, 109-66-0; hexane, 110-54-3; heptane, 142-82-5; octane, 111-65-9.

(31) Rosenstock, H. M.; Draxl, K.; Steiner, D. W.; Herron, J. T. *J. Phys. Chem. Ref. Data, Suppl.* **1977**, *6*.

(32) Sequential loss of H_2 and an alkene will also yield products corresponding to alkane loss. Due to energetics, however, we believe direct alkane loss to be the dominant process.

(33) Auxiliary heats of formation are taken from: Cox, J. D. Pilcher, G. "Thermochemistry of Organic and Organometallic Compounds"; Academic Press: New York, 1970.